



ELSEVIER

Journal of Immunological Methods 283 (2003) 291–306

JIM
Journal of
Immunological Methods

www.elsevier.com/locate/jim

Recombinant Technology

Accurate and statistically verified quantification of relative mRNA abundances using SYBR Green I and real-time RT-PCR

Julie H. Marino^{a,b}, Peyton Cook^c, Kenton S. Miller^{a,b,*}

^aFaculty of Biological Sciences, The University of Tulsa, 600 S. College Avenue, Tulsa, OK 74104-3189, USA

^bMervin Bovaird Center for Studies in Molecular Biology and Biotechnology, The University of Tulsa, Tulsa, OK 74104-3189, USA

^cDepartment of Mathematical and Computer Sciences, The University of Tulsa, Tulsa, OK 74104-3189, USA

Received 25 April 2002; received in revised form 16 July 2002; accepted 7 January 2003

Abstract

Among the many methods currently available for quantifying mRNA transcript abundance, reverse transcription-polymerase chain reaction (RT-PCR) has proved to be the most sensitive. Recently, several protocols for real-time relative RT-PCR using the reporter dye SYBR Green I have appeared in the literature. In these methods, sample and control mRNA abundance is quantified relative to an internal reference RNA whose abundance is known not to change under the differing experimental conditions. We have developed new data analysis procedures for the two most promising of these methodologies and generated data appropriate to assess both the accuracy and precision of the two protocols. We demonstrate that while both methods produce results that are precise when 18S rRNA is used as an internal reference, only one of these methods produces consistently accurate results. We have used this latter system to show that mRNA abundances can be accurately measured and strongly correlate with cell surface protein and carbohydrate expression as assessed by flow cytometry under different conditions of B cell activation.

© 2003 Elsevier B.V. All rights reserved.

Keywords: B lymphocyte; RT-PCR; mRNA; SYBR Green; Smart Cycler

1. Introduction

1.1. Quantitative RT-PCR

It is frequently useful in both the research and clinical settings to be able to quantify changes in mRNA transcript abundance, and over the years, many immunologically relevant applications for

Northern blotting, in situ hybridization, and RNase protection assays have been published. The discovery of the polymerase chain reaction (PCR) by Mullis et al. (1986) opened the door for the use of this powerful technique in the analysis of mRNA abundances using reverse-transcribed RNA (RT-PCR); however, development of the quantitative aspects of this application has been hampered by its sensitivity (Freeman et al., 1999). Recently, the advent of automated methods for following PCR progress by measuring fluorescence increase in real time has significantly extended the potential of RT-PCR for quantitative applications (Higuchi et al., 1993; Wittwer et al., 1997), and many

* Corresponding author. Tel.: +1-918-631-3065; fax: +1-918-631-2762.

E-mail address: Kenton-Miller@utulsa.edu (K.S. Miller).

different experimental approaches have been developed toward this end (for examples, see Blaschke et al., 2000; Kruse et al., 2001; Hempel et al., 2002). Such applications have been shown to more or less accurately quantify absolute numbers of mRNA transcripts per cell with a 10,000- to 100,000-fold increase in sensitivity compared to RNase protection assays (Wang and Brown, 1999; for a recent review, see Bustin, 2000).

More frequently, however, knowledge of absolute numbers of transcripts is not required to answer the question at hand, and it is sufficient to document changes in the relative abundance of a specific transcript or transcripts between varying experimental or developmental conditions. In different discussions, this process has been termed either “relative quantitative” or “semiquantitative” RT-PCR. Several procedures for analyzing and validating data from such experiments have been published (Muller et al., 2002; Liu and Saint, 2002; Livak and Schmittgen, 2001; Pfaffl, 2001; Gentle et al., 2001). As pointed out by Muller et al., the calculation of mean normalized gene expression can be performed in any of several different ways, each of which can yield different results and lead to very different estimates of standard error. Thus, the issue of how best to calculate these values is yet unresolved.

For the sake of clarity in the subsequent discussion, we will briefly recapitulate the commonly accepted mathematical ideas used in analyzing relative RT-PCR reactions.

1.2. The mathematics of PCR

Product accumulation during the early stages of a PCR reaction may be modeled using the equation for density-independent population growth in discrete time, which is:

$$N_{t+1} = mN_t,$$

where N_t is the population size at time t , N_{t+1} is the population size at time t plus 1 interval, and m is population growth rate per interval. A PCR reparameterized solution of this equation is:

$$N = N_0 E^C, \quad (1)$$

where N_0 is the number of target DNA molecules (amplicons) at the beginning of the reaction, N is the number of amplicons at the end of cycle number C , and E is the efficiency of the reaction, which in theory is a number between 1 and 2. In order to make E consistent with the concept of efficiency, usually expressed as a number between 0 and 1 or as a percentage, the expression $(1+E)$ is frequently used in place of E in Eq. (1) (Freeman et al., 1999). Such notation leads to unnecessary complications when one is attempting to derive secondary formulae from Eq. (1) and we have therefore avoided its use.

In relative RT-PCR, one is normally only concerned with the ratio (R) of the initial amplicon abundance of a specific mRNA between two experimentally distinct cDNA populations, N_{o1} and N_{o2} , herein called the sample and control populations, respectively. Thus,

$$R = (N_{o1}/N_{o2}). \quad (2)$$

Consolidating Eqs. (1) and (2) and taking the natural logarithm of each side to linearize the resultant equation, we have:

$$\ln R = (\ln N_1 - C_1 \ln E_1) - (\ln N_2 - C_2 \ln E_2).$$

At any particular $N_1 = N_2$, i.e. when the amplicon population growth has reached an identical point in each PCR reaction,

$$\ln R = C_2 \ln E_2 - C_1 \ln E_1.$$

At this point, it is usually assumed that the amplification efficiency of the amplicon for the two cDNA populations is equal ($E_1 = E_2$). Then and only then,

$$\ln R = \Delta C \ln E, \quad (3)$$

and

$$R = E^{\Delta C} \quad (4)$$

The ΔC in Eq. (4) is then the experimentally determined difference between the cycle numbers (C_i) at which each of the two PCR reactions attains some arbitrary threshold number of detectable amplicons (i.e. $\Delta C = C_{t2} - C_{t1}$, where $N_1 = N_2 =$ the threshold value).

The abundance ratio (R) for the two mRNA populations must also be corrected for differences in the yields between the two reverse transcriptase reactions. When this final correction is made, we obtain the final ratio that we will here call R^* . Such calibrations are normally accomplished using a second, internal reference amplicon whose abundance is believed not to change appreciably between the varying experimental conditions under consideration (Livak and Schmittgen, 2001; however, see also Thellin et al., 1999).

If both the sample/control amplicon and the internal reference amplicon are kept small (≤ 150 bp), and all PCR reactions are rigorously optimized, then the so-called $2^{-\Delta\Delta C_t}$ method may be used (Sagner and Goldstein, 2001; Livak and Schmittgen, 2001). In this method, all amplicon efficiencies are assumed to be at the theoretical maximum value of 2. However, in practice, this is usually not the case, and recently, Pfaffl (2001) described a new mathematical approach for determining the corrected ratio that does not assume equal or optimal efficiencies for either amplicon.

1.3. The importance of accurate efficiency determinations

Because of the exponential relationship between R and E (see Eq. (4) above), small errors in the experimental determination of E or C can have very large effects on the apparent value of R . Thus, the best method for evaluating both E and C is a matter of import. Recently, two very different protocols for determining E have appeared in the literature. One of these methods (Pfaffl, 2001), which we call the standard curve method, relies on the production and use of standard curves, whereas the other, which we call the analytical method, determines efficiency from analysis of the same data set used to determine the C_t (Gentle et al., 2001). We have modified the approach of Gentle et al. and developed new statistical equations for rigorous quantitative analysis using either method. We then used these equations to assess both the precision and the accuracy of each method using mRNA populations from differentially activated B cells as a model system. We show that while both methods are precise, the analytical method is significantly the more accurate when data from RT-PCR reactions performed on different days is analyzed. Finally, we show that our analytical method allows

the relative quantification of mRNA populations that is rapid, precise, accurate, and statistically validated. Further, this approach should be easily adaptable to a variety of instruments and detection systems.

2. Materials and methods

2.1. Animal strains

C57BL/6 mice originally purchased from Jackson Laboratories (Bar Harbor, ME), have been bred and maintained in the University of Tulsa Animal Facility. All mice used were females of at least 6 weeks of age.

2.2. Preparation and analysis of small resting B cells

Pure B cells were isolated and analyzed by the method previously described (Bagriacik and Miller, 1999). Briefly, murine splenic cells were treated with an ammonium chloride lysis to remove red blood cells, and complement mediated lysis was used to eliminate macrophages and T cells. Ficoll gradients were used to isolate viable high-density resting B cells.

2.3. In vitro activation of B cells

B cells were cultured in 24 well plates at 5×10^6 cells/ml. For activation through cross-linking of cell surface IgM, 5 $\mu\text{g/ml}$ of goat anti-mouse IgM F(ab')₂ (Jackson Immunoresearch Laboratories, West Grove, PA), 15 ng/ml of recombinant IL-2 (Sigma-Aldrich, St. Louis, MO), and 5 ng/ml of mouse recombinant IL-4 (Sigma-Aldrich) were added prior to culture. Activation was also obtained by the use of 1 $\mu\text{g/ml}$ of anti-mouse CD40 (BD Biosciences Pharmingen, San Diego, CA) along with 15 ng/ml of recombinant IL-2. Cells were incubated with the appropriate stimulatory molecules in RPMI-1640 supplemented with L-glutamine, 2-mercaptoethanol, antibiotics, and 10% heat-inactivated fetal calf serum at 37 °C in a humidity-controlled incubator and 10% CO₂ for 48 h prior to harvesting.

2.4. RNA isolation

RNA was prepared from cell suspensions using TRIzol Reagent (Gibco BRL, Gaithersburg, MD)

according to the manufacturers' instructions. Quality and quantity of RNA was assessed by measuring the A_{260}/A_{280} ratio and by analysis on ethidium bromide stained 1% agar gels with and without heating to 65 °C for 10 min in sterile, diethyl pyrocarbonate-treated, 18 MΩ water. Gels were imaged on a Molecular Dynamics Storm and analyzed using ImageQuant software (Amersham Pharmacia Biotech, Piscataway, NJ). Any RNA preparations exhibiting significant qualitative or quantitative differences between heated and unheated samples were rejected. Isolated RNA was treated with DNase I (Invitrogen, Carlsbad, CA) prior to use for cDNA synthesis.

2.5. cDNA synthesis, RNase H treatment, and PCR amplification

Reverse transcription was performed using 5 µg of total RNA, random primers, and SuperScript II RT (Invitrogen) in a total volume of 20 µl. The reaction was incubated at 25 °C for 10 min followed by incubation at 42 °C for 50 min. cDNA synthesis was followed by RNase H treatment (Roche Molecular Biochemicals, Indianapolis, IN). To minimize potential effects of differential synthesis during the RT reaction, three separate cDNA reactions were pooled for each RNA preparation analyzed. Real-time PCR was carried out using a Smart Cycler thermal cycler (Cepheid, Sunnyvale, CA). Each PCR reaction included 2.5 µl of 10 × PCR Buffer without MgCl₂ (Sigma-Aldrich), 1.0 µl of 25 mM MgCl₂, 0.5 µl of 10 mM dNTPs (Perkin-Elmer, Wellesley, MA), 20 pM each primer, 0.25 µl of Taq DNA Polymerase (Sigma-Aldrich), 0.2 µl of 30% BSA (Sigma-Aldrich), SYBR Green I (Molecular Probes, Eugene, OR) at a final dilution of 1:20,000 of the commercial stock, and an appropriate volume of the cDNA preparation. PCR cycling conditions included a 94 °C heating step for 1 min at the beginning of every run. The tubes were then cycled at 94 °C for 30 s, annealed at 62–68 °C for 60 s, and extended at 72 °C for 60 s. Optical data was collected during the annealing step. A melting curve was generated at the end of every run to ensure product uniformity (Ririe et al., 1997). Primers for PCR: 18S rRNA forward: 5'-TCAAGAAGAAAGTTCGGAGGTT-3'; 18S rRNA reverse: 5'-GGACATCTAAGGGCATCACAG-3'; murine β-actin

forward: 5'-CAGCTTCTTTGCAGCTCCTT-3'; murine β-actin reverse: 5'-TCACCCACATAGGAGTCCTT-3'; murine CD80-forward: 5'-TGAAATGATGAGTCTGAAGACCGAATC-3'; murine CD80-reverse: 5'-TTCCTCTTTCCTTCTTTTGAACGAC-3'; murine ICAM-1 forward: 5'-CC-TGCCTCTGAAGCTCGGATA-3'; murine ICAM-1 reverse: 5'-CTAAAGGCATGGCACACGTATGTA-3'; murine ST3Gal I forward: 5'-GGAGGAGGACACATACCGGTG-3'; murine ST3Gal I reverse: 5'-GGA-GTCCTTCAGGTTACCGGAG-3'; murine ST3Gal V forward: 5'-TATGTGGACCCTGACCGGAT-3'; murine ST3Gal V reverse: 5'-GGCGTAGTATTCAA-CGTCCGA-3'. The 18S rRNA, CD80, ICAM-1, ST3Gal I, and ST3Gal V primers were synthesized by the Recombinant DNA/Protein Resource Facility at Oklahoma State University (Stillwater, OK). Murine β-actin primers were purchased from Midland Certified Reagent Co., (Midland, TX).

2.6. Cell staining with monoclonal antibodies

Cells were stained as described previously (Bagriacik and Miller, 1999). All antibodies were purchased from BD Biosciences Pharmingen. Briefly 1×10^6 cells were incubated with Fc receptor block (anti-CD16/32), and then stained with biotin-conjugated anti-mouse CD54 (ICAM-1) or biotinylated anti-mouse CD80 (B7-1) followed by streptavidin-PE. Staining and washing of cells were performed in monoclonal antibody wash (Hanks Balanced Salts, 1% BSA, and 0.01% sodium azide). Stained cells were analyzed on an EPICS 751 flow cytometer interfaced with a Cicero data acquisition unit. List mode data was analyzed with Cyclops software (Cytomation, Fort Collins, CO).

2.7. Data analysis

For analysis by the analytical method of Gentle et al. (2001), optics data was exported from the Cepheid Smart Cycler as comma separated values files (*.csv) and imported into MS Excel. We have written a Visual Basic Excel macro that facilitates determination and conversion of the appropriate Smart Cycler optics data to a logarithmic format for subsequent analysis. The resultant data was then pasted into SAS JMPIN 4.0 for determination of slopes, intercepts, and their respec-

tive standard errors and correlation coefficients, which were subsequently pasted into a second MS Excel spreadsheet designed to calculate \hat{R} and \hat{R}^* .

For analysis by the standard curve method of Pfaffl (2001), C_t data was exported from the Cepheid Smart Cycler as comma separated values files (*.csv) and imported into MS Excel. The appropriate data was then pasted into a GraphPad Prism spreadsheet for linear regression analysis and for determining mean C_t values. These values and their corresponding standard errors were then pasted into yet another MS Excel spreadsheet designed to calculate \hat{R} and \hat{R}^* by the method of Pfaffl. All Excel spreadsheets and macros are available upon request to the corresponding author.

3. Results

3.1. A statistically significant day effect

Although others have reported on the precision of real-time RT-PCR data, previous reports have used either: (1) highly purified double-stranded DNA as an analog for cDNA from a reverse transcriptase reaction (Gentle et al., 2001); (2) a prokaryotic model in which mRNA population complexity is relatively low and induction ratios are relatively high (Pfaffl, 2001); or (3) a significantly different detection system such as a TaqMan probe (Overbergh et al., 1999). Here we show that when using SYBR Green I for detection, inter- and intra-assay precision can be high, but there are caveats that cannot be ignored and therefore must be incorporated into any experimental design (see below).

To determine inter- and intra-assay variability, four individual reaction mixes containing β -actin specific primers were prepared and each reaction mix was aliquoted into four sample tubes. Each of the 16 samples was cycled through 40 cycles, the growth curves were monitored, and the C_t of each reaction was determined (Fig. 1A). One-way ANOVA analysis showed that the reaction mixes were not significantly different ($p > 0.1$). Further, when all data groups were combined, the data was normally distributed (KS distance = 0.105). We interpret this to mean that when due care is taken, multiple reaction mixes made from the same reagents on the same day

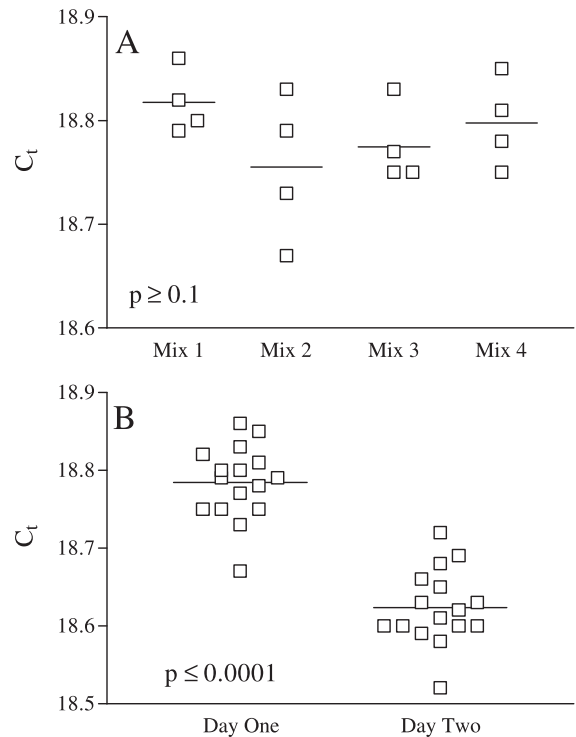


Fig. 1. (A) PCR was performed on four aliquots each of four separate reaction mixes. Each reaction mix contained identical amounts cDNA from anti-CD40-stimulated murine B-lymphocytes and β -actin primers. The reactions were run for 40 cycles in the Smart Cycler and second derivative C_t data was collected. One-way ANOVA analysis showed that the C_t data was not significantly different ($p > 0.1$). (B) The next day, the eight PCR reactions were repeated exactly as in (A). The C_t data from the two days was compared by ANOVA and found to be significantly different ($p < 0.0001$). This experiment has been repeated several times with similar results.

are equivalent and thus comparable. Since the data was normally distributed, we evaluated various size groupings to determine the minimum size necessary for a routine precision of ± 0.1 cycle. As previously reported by Gentle et al. (2001), this turned out to be six replicates.

When the experiment was repeated the next day using the same stock reagents, similar results with respect to inter- and intra-assay variance were observed; however, when the grouped data was compared to the grouped data from the previous day, a small but statistically significant day effect was observed (Fig. 1B). We have been unable to identify

any one particular origin for this effect, and its occurrence, amplitude, and direction of change are variable; however, it is probably the result of minute changes in the initial conditions of the reaction mix due to pipetting inaccuracies, etc.

When examining the variance of C_t among replicates, one must keep in mind that C_t is determined from a log-linear plot and is thus an exponential function. To get accurate coefficients of variation, the data must be linearized (Livak and Schmittgen, 2001). To assess the real error introduced by the day effect on this particular day (in this case, the mean difference was 0.16 cycles), we linearized the data by assuming an efficiency for the reaction of two ($E=2$) and setting $\Delta C=0.16$ in Eq. (4) from Introduction. This results in an apparent 12% difference in actin abundance between two aliquots of an identical cDNA population. The existence of this effect means that using data collected on different days for the calculation of an R -value will introduce variable and statistically significant errors that are uncontrolled and undeterminable. When normalizing, any such errors will be propagated and amplified as well. Thus, for maximum accuracy, all data for individual target/reference pairs must be obtained on the same day using a single reaction mix.

3.2. The internal reference amplicon

R and, subsequently, R^* depend not only on the PCR reaction conditions, but, as noted in Introduction, also depend on the exact amount of input RNA and on the yield of the reverse transcriptase (RT) reactions. Among the many internal reference amplicons that have been used previously, we chose to normalize our PCR reactions to the amount of 18S rRNA sequence in the synthesized cDNA. We do this for several reasons. First, a preliminary PCR for 18S rRNA sequences provides a rapid estimation for

the correct amount of RT mix to add to subsequent PCR reactions. In our experience, 18S rRNA should have a C_t no greater than 15 cycles if low abundance transcripts are to be amplified above what turns out to be a lower level for effective detection with SYBR Green I of around 35 cycles. Above this level, false priming and or primer–dimer formation due to the presence of SYBR Green I may significantly interfere with C_t determination in a primer-dependent manner (data not shown). When using TaqMan or molecular beacon probes, this should not present a problem; however, these approaches are significantly more expensive and less versatile. Second, 18S rRNA is probably a more representative measure of total RNA than either GAPDH or β -actin (Goidin et al., 2001; Schmittgen and Zakrajsek, 2000; however, see also Spanakis, 1993). Finally, because there are hundreds of copies of the rRNA gene, it is a very sensitive marker for genomic DNA contamination of our RNA preparations if detected in RT^{minus} controls.

3.3. Equations for relative RT-PCR

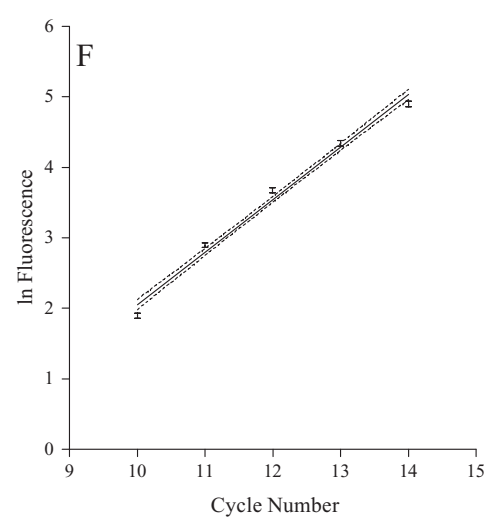
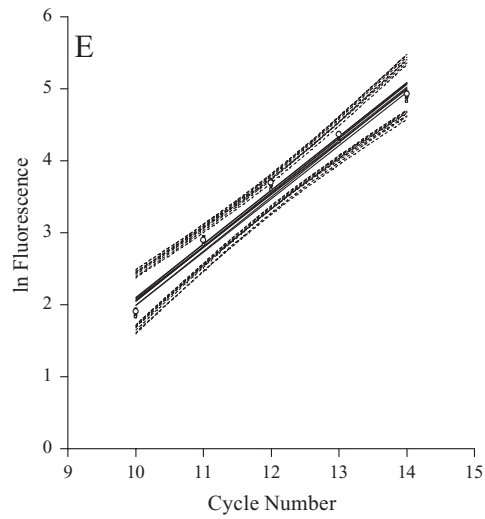
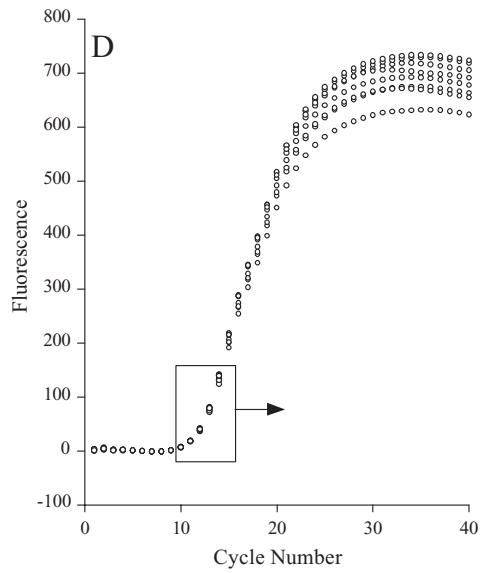
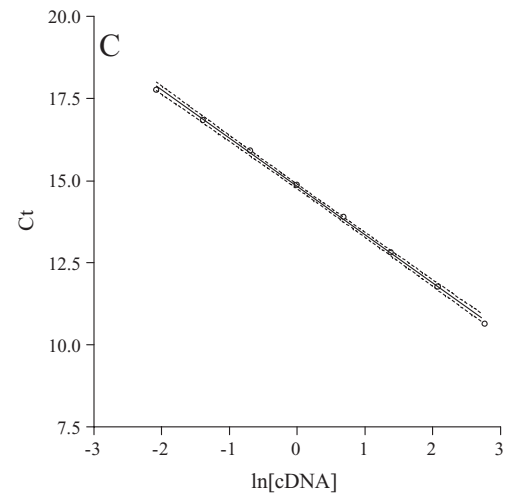
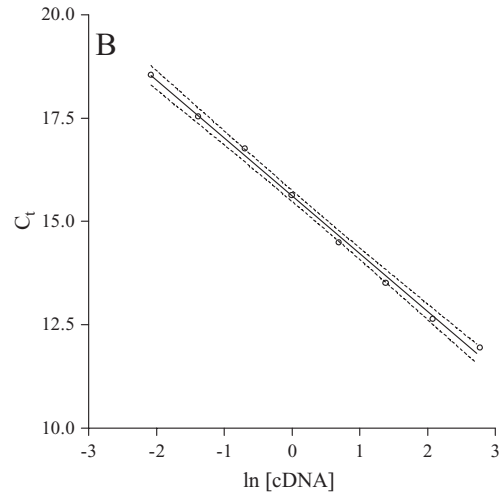
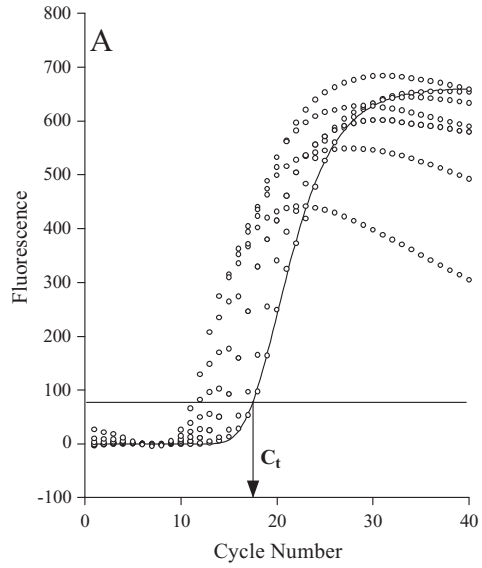
3.3.1. Determination of PCR reaction efficiency by the standard curve method—Pfaffl (2001)

Although not explicitly stated in his paper, to determine efficiency by the standard curve method, one takes the logarithm of Eq. (1) in Introduction and rearranges to obtain:

$$C = (-1/\ln E)\ln N_0 + (1/\ln E)\ln N.$$

After running RT-PCR reactions on a dilution series of the cDNA (Fig. 2A), one plots threshold cycle number (C_t) against the logarithm of the initial cDNA concentration ($\ln N_0$) to get a linear plot in which the slope is equal to $-1/\ln E$ (Fig. 2B and C).

Fig. 2. PCR was performed on aliquots of a 2-fold dilution series of a cDNA from anti-CD40-stimulated murine B-lymphocytes using primers specific for 18S ribosomal RNA. Amplicon abundance was monitored in real time by measuring SYBR Green I fluorescence (A). C_t values determined either by the threshold method (B) as illustrated in (A) or by the second derivative method (C) were plotted against the natural logarithm of the cDNA concentration in the reaction mix. Alternatively, PCR was performed on eight identical aliquots of the cDNA mix in (A) and amplicon abundance was monitored (D). The natural logarithm of the fluorescence at each cycle within the log-linear portion of the growth curve (boxed in D) was then plotted against the cycle number (E), or else, the mean of those determinations was plotted (F). The dotted lines in B, C, E, and F represent the 95% confidence intervals of the regression lines. The efficiency, E , of the reaction was determined from the slope of the appropriate regression line either as $E = e^{-1/\text{slope}}$ (B, C) or as $E = e^{\text{slope}}$ (F).



3.3.2. Determination of PCR reaction efficiency by the analytical method—Gentle et al. (2001)

Again, although not explicitly stated in their paper, in the analytical method, one takes the logarithm of Eq. (1) as above and rearranges to obtain:

$$\ln N = (\ln E)C + \ln N_0.$$

Using SYBR Green I, fluorescence is a linear function of the DNA concentration. Thus, after running RT-PCR reactions on a series of replicates (Fig. 2D), a plot of the natural logarithm of the fluorescence versus the cycle number (Fig. 2E and F) for the early, log-linear portion of the curve has a slope that is equal to $\ln E$. The anti-log of the slope of this plot is then the efficiency of the reaction.

3.3.3. Equations for determining R and the variance of R by the standard curve method

Using Eq. (3) from Introduction and the relationship between slope (β) and efficiency (E) defined in the standard curve method ($\ln E = -1/\beta$), we can derive the following equations for determining the natural logarithm of the estimated R-value ($\ln \hat{R}$) and its associated variance ($\hat{\text{var}}_{\ln \hat{R}}$). Thus:

$$\ln \hat{R} = \frac{\hat{C}_{12} - \hat{C}_{11}}{\hat{\beta}}, \tag{6}$$

and

$$\hat{\text{var}}_{\ln \hat{R}} \approx \left(\frac{\hat{\sigma}_{\hat{C}_{11}}}{\hat{\beta}}\right)^2 + \left(\frac{\hat{\sigma}_{\hat{C}_{12}}}{\hat{\beta}}\right)^2 + \left(\frac{(\hat{C}_{12} - \hat{C}_{11})\hat{\sigma}_{\hat{\beta}}}{\hat{\beta}^2}\right)^2 \tag{7}$$

where $\hat{\beta}$ and $\hat{\sigma}_{\hat{\beta}}$ are the mean least squares slope and standard error from the efficiency determination, and \hat{C}_{11} , \hat{C}_{12} and $\hat{\sigma}_{\hat{C}_{11}}$, $\hat{\sigma}_{\hat{C}_{12}}$ are the mean C_t -values and standard errors determined for each of the two cDNA populations under consideration, respectively.

3.3.4. Equations for determining R and the variance of R by the analytical method

Because the slope and the C_t are determined from the same set of data, the analytical method requires a considerably more complicated mathematical ap-

proach to the determination of variance than that reported by Gentle et al. (2001). The C_t values must first be defined in terms of some threshold value (t), mean slope ($\hat{\beta}$), and mean y-intercept ($\hat{\alpha}$) of a mean regression line through the data points, as shown in Fig. 3. Thus, for cDNA₁ and cDNA₂, one can write:

$$t = \hat{\alpha}_1 + \hat{\beta}_1 \hat{C}_{t1} \Rightarrow \hat{C}_{t1} = \frac{t - \hat{\alpha}_1}{\hat{\beta}_1}, \text{ and}$$

$$t = \hat{\alpha}_2 + \hat{\beta}_2 \hat{C}_{t2} \Rightarrow \hat{C}_{t2} = \frac{t - \hat{\alpha}_2}{\hat{\beta}_2}$$

where $\hat{\beta}_1$, $\hat{\alpha}_1$ and $\hat{\beta}_2$, $\hat{\alpha}_2$ are the mean slopes and intercepts from the two linear regressions, respectively. Finally, mean slopes and intercepts with standard errors are calculated from the data points for each experimental condition, and a covariance for the slope and intercept is determined. We can average the mean

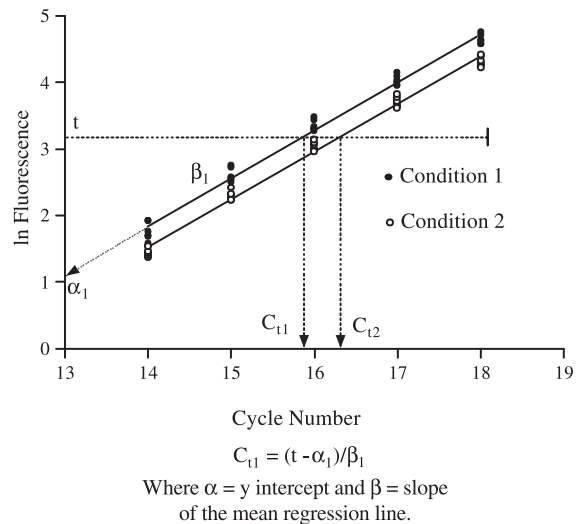


Fig. 3. To demonstrate our method of analysis, PCR was performed with actin primers on six aliquots each of two reaction mixes containing cDNA from two different anti-CD40-stimulated B-lymphocyte preparations. The reactions were run for 40 cycles in the Smart Cycler and fluorescence data was collected. The natural logarithm of the fluorescence was calculated for each data point, and the linear portion of the graph of $\ln F$ versus cycle number was determined. A linear regression analysis was then performed on that data subset considered as a whole. A C_t value for each preparation that is dependent on the calculated slope (β) and intercept (α) of the mean regression line can now be defined for any predefined threshold value (t).

slope data (i.e. $\ln E = 1/2(\beta_1 + \beta_2)$) and combine this with Eq. (3) from Introduction to write:

$$\ln \hat{R} = \frac{1}{2} \left(\frac{t - \hat{\alpha}_1}{\hat{\beta}_1} - \frac{t - \hat{\alpha}_2}{\hat{\beta}_2} \right) (\hat{\beta}_1 + \hat{\beta}_2), \quad (8)$$

and

$$\begin{aligned} \hat{\text{var}}_{\ln \hat{R}} \approx & \left(-\frac{\hat{\beta}_1 + \hat{\beta}_2}{2\hat{\beta}_1} \right)^2 \hat{\sigma}_{\hat{\alpha}_1}^2 + \left(-\frac{(\hat{\beta}_1 + \hat{\beta}_2)(t - \hat{\alpha}_1)}{2\hat{\beta}_1^2} \right. \\ & + \left. \frac{1}{2} \left(\frac{t - \hat{\alpha}_1}{\hat{\beta}_1} - \frac{t - \hat{\alpha}_2}{\hat{\beta}_2} \right) \right)^2 \hat{\sigma}_{\hat{\beta}_1}^2 \\ & + 2 \left(-\frac{\hat{\beta}_1 + \hat{\beta}_2}{2\hat{\beta}_1} \right) \left(-\frac{(\hat{\beta}_1 + \hat{\beta}_2)(t - \hat{\alpha}_1)}{2\hat{\beta}_1^2} \right. \\ & + \left. \frac{1}{2} \left(\frac{t - \hat{\alpha}_1}{\hat{\beta}_1} - \frac{t - \hat{\alpha}_2}{\hat{\beta}_2} \right) \right) \text{cov}(\hat{\alpha}_1, \hat{\beta}_1) \\ & + \left(\frac{\hat{\beta}_1 + \hat{\beta}_2}{2\hat{\beta}_2} \right)^2 \hat{\sigma}_{\hat{\alpha}_2}^2 + \left(\frac{(\hat{\beta}_1 + \hat{\beta}_2)(t - \hat{\alpha}_2)}{2\hat{\beta}_2^2} \right. \\ & + \left. \frac{1}{2} \left(\frac{t - \hat{\alpha}_1}{\hat{\beta}_1} - \frac{t - \hat{\alpha}_2}{\hat{\beta}_2} \right) \right)^2 \hat{\sigma}_{\hat{\beta}_2}^2 \\ & + 2 \left(\frac{\hat{\beta}_1 + \hat{\beta}_2}{2\hat{\beta}_2} \right) \left(\frac{(\hat{\beta}_1 + \hat{\beta}_2)(t - \hat{\alpha}_2)}{2\hat{\beta}_2^2} \right. \\ & + \left. \frac{1}{2} \left(\frac{t - \hat{\alpha}_1}{\hat{\beta}_1} - \frac{t - \hat{\alpha}_2}{\hat{\beta}_2} \right) \right) \text{cov}(\hat{\alpha}_2, \hat{\beta}_2). \quad (9) \end{aligned}$$

3.3.5. Equations for calculation of the corrected ratio \hat{R}^* with associated confidence interval

To calculate the corrected difference in sequence abundance between two cDNAs (\hat{R}^*), we must determine a second \hat{R} -value for an internal reference RNA and use this value to normalize for differences in the efficiency of the reverse transcriptase reaction, i.e. $\hat{R}^*_{\text{Target}} = \hat{R}_{\text{Target}} / \hat{R}_{\text{Reference}}$. The easiest way to calculate the normalized ratio is to recognize that:

$$\ln \hat{R}^*_{\text{Target}} = \ln \hat{R}_{\text{Target}} - \ln \hat{R}_{\text{Reference}},$$

and

$$\hat{\text{var}}_{\ln \hat{R}^*_{\text{Target}}} \approx \hat{\text{var}}_{\ln \hat{R}_{\text{Target}}} + \hat{\text{var}}_{\ln \hat{R}_{\text{Reference}}}$$

The 95% confidence interval is then:

$$\ln \hat{R}^*_{\text{Target}} \pm z_{0.25\%} \sqrt{\hat{\text{var}}_{\ln \hat{R}^*_{\text{Target}}}}$$

We have designed MS Excel spreadsheets that significantly simplify data entry and automate the process of calculating \hat{R}^* for both the standard curve method and the analytical method.

3.4. Proof of principle

Although the standard curve method is the simplest and, under the proper conditions, most precise method available, it requires the use of a significant number of extra data points for the determination of E . Further, there is the explicit assumption that a given amplicon will always amplify with efficiency identical to that determined by the dilution analysis, i.e. efficiency is experimental-condition-independent; however, this may not always be the case (Liu and Saint, 2002, and our unpublished results). For these reasons alone, the analytical method might be preferable if it could be demonstrated to produce results at least as precise and accurate as those of the standard curve method.

As shown in Fig. 4, B cells activated via CD40 cross-linking express significantly more ICAM-1 and CD80 on their surface than do B cells activated via sIgM cross-linking. We purified total RNA from each of these populations and defined the cDNA from the anti-IgM-activated cells as the control and the cDNA from the anti-CD40-activated cells as the sample. We then assessed the relative amounts of β -actin, ICAM-1, and CD80 by the standard curve method (Table 1) and the analytical method (Table 2) as described above, using 18S rRNA as the internal reference.

Both methods reported significantly more β -actin in the anti-CD40-activated cells relative to the anti-IgM-activated cells ($\hat{R}^* = 2.6$ for both methods). Both methods were consistent in reporting significantly increased amounts of mRNA for both ICAM-1 ($\hat{R}^* = 5.1$ and 4.8, respectively) and CD80 ($\hat{R}^* = 15.3$ and 12.8, respectively) in the anti-CD40-activated sample. Such increases are consistent with the increased amount of these proteins observed on the anti-CD40 cell surface via flow cytometry (Fig. 4). It is clear, however, that the results given by the two methods increasingly deviate from each other as the difference in the abundance between the sample and

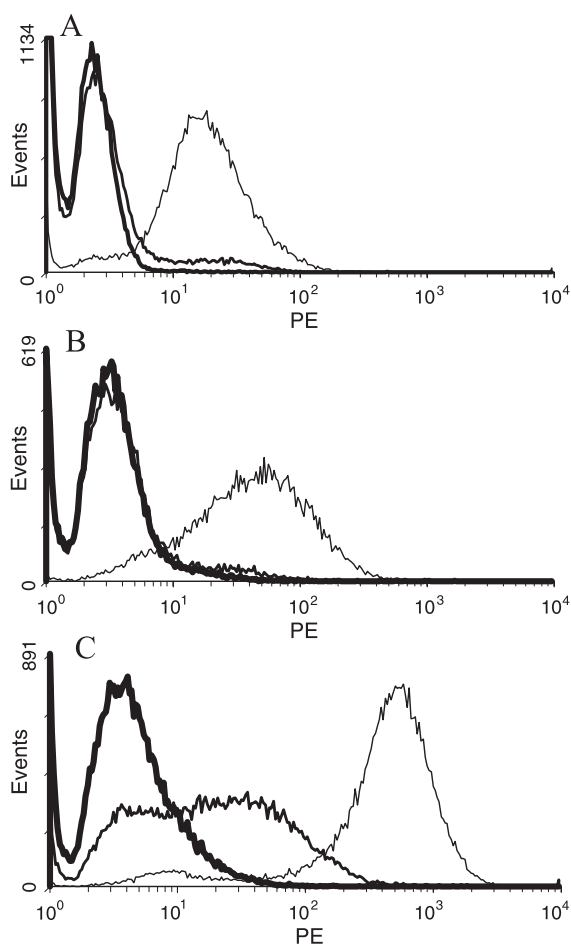


Fig. 4. B-lymphocytes were prepared as in Materials and methods and resting cells (A), cells activated with anti-IgM (B), and cells activated with anti-CD40 (C) were stained with biotinylated monoclonals for anti-TNP (isotype control—thick line), anti-CD80 (medium line), and anti-ICAM-1 (thin line), then counterstained with phycoerythrin (PE)-conjugated streptavidin. Fluorescence of live cells was measured following gating on the appropriate population of a FALS/90 plot.

control populations increased. Since both could not be simultaneously correct, we wondered whether we could distinguish which, if either, of the two methods was the most accurate.

3.5. A method to estimate accuracy

Having established that our equations gave reasonable results, but concerned that one or both of the experimental methods did not produce accurate

results, we tested both methods for sensitivity to the ‘day effect’ by deriving \hat{R}^* values for the same cDNA analyzed on two different days separated by several weeks. Under these conditions, we expect \hat{R}^* to be 1.0 because the sample and control cDNA populations are identical. Since the \hat{R}^* value for CD80 mRNA abundance showed the greatest divergence between the two methods, we chose it along with two other low abundance mRNAs (ST3Gal I and ST3Gal V) for the analysis. As shown in Table 3, the standard curve method again produced a precise result but with a significant and variable inaccuracy (1.6, 0.9, and 0.7). On the other hand, the analytical method produced both a precise and very accurate result (1.0 when rounded to one decimal place for all genes tested).

We conclude that the analytical method gives a more accurate result because all calculated values for E and C are derived from a single data set, whereas

Table 1
The standard curve method

18S					Relative mRNA abundance (α CD40/ α IgM)
$\hat{\beta}$	$\hat{\sigma}_{\hat{\beta}}$	\hat{C}_{11}	$\hat{\sigma}_{\hat{C}_{11}}$	$\ln \hat{R}^* =$	Actin
-1.520	0.027	12.313	0.015	0.065	$\hat{R}^* = 2.6$
		\hat{C}_{12}	$\hat{\sigma}_{\hat{C}_{12}}$	$\hat{\text{var}}_{\ln \hat{R}^*} =$	L CI _{95%} = 2.3
		12.214	0.024	0.0004	U CI _{95%} = 2.9
Actin					ICAM-1
$\hat{\beta}$	$\hat{\sigma}_{\hat{\beta}}$	\hat{C}_{11}	$\hat{\sigma}_{\hat{C}_{11}}$	$\ln \hat{R}^* =$	$\hat{R}^* = 5.1$
-1.529	0.014	17.359	0.055	1.015	L CI _{95%} = 4.7
		\hat{C}_{12}	$\hat{\sigma}_{\hat{C}_{12}}$	$\hat{\text{var}}_{\ln \hat{R}^*} =$	U CI _{95%} = 5.5
		15.808	0.072	0.001	
ICAM-1					CD80
$\hat{\beta}$	$\hat{\sigma}_{\hat{\beta}}$	\hat{C}_{11}	$\hat{\sigma}_{\hat{C}_{11}}$	$\ln \hat{R}^* =$	$\hat{R}^* = 15.3$
-1.528	0.008	24.299	0.052	1.685	L CI _{95%} = 12.9
		\hat{C}_{12}	$\hat{\sigma}_{\hat{C}_{12}}$	$\hat{\text{var}}_{\ln \hat{R}^*} =$	U CI _{95%} = 18.0
		21.724	0.024	0.007	
CD80					
$\hat{\beta}$	$\hat{\sigma}_{\hat{\beta}}$	\hat{C}_{11}	$\hat{\sigma}_{\hat{C}_{11}}$	$\ln \hat{R}^* =$	
-1.405	0.037	27.391	0.043	2.790	
		\hat{C}_{12}	$\hat{\sigma}_{\hat{C}_{12}}$	$\hat{\text{var}}_{\ln \hat{R}^*} =$	
		23.471	0.013	0.007	

Table 2
The analytical method

18S						Relative mRNA abundance (α CD40/ α IgM) Actin
$\hat{\beta}_1$	$\hat{\sigma}_{\hat{\beta}_1}$	$\hat{\alpha}_1$	$\hat{\sigma}_{\hat{\alpha}_1}$	cov($\hat{\beta}_1, \hat{\alpha}_1$)	$t=1.5$ $\ln \hat{R}=0.077$ $\hat{\text{var}}_{\ln \hat{R}}=0.0005$	
0.658	0.011	-7.130	0.142	-0.002		
$\hat{\beta}_2$						
0.646	0.011	-6.900	0.149	-0.002		
Actin						
$\hat{\beta}_1$	$\hat{\sigma}_{\hat{\beta}_1}$	$\hat{\alpha}_1$	$\hat{\sigma}_{\hat{\alpha}_1}$	cov($\hat{\beta}_1, \hat{\alpha}_1$)	$t=1.5$ $\ln \hat{R}=1.036$ $\hat{\text{var}}_{\ln \hat{R}}=0.001$	$\hat{R}^*=2.6$ L CI _{95%} =2.4 U CI _{95%} =2.8
0.645	0.013	-10.181	0.230	-0.003		
$\hat{\beta}_2$						
0.672	0.017	-9.609	0.268	-0.004		
ICAM-1						
$\hat{\beta}_1$	$\hat{\sigma}_{\hat{\beta}_1}$	$\hat{\alpha}_1$	$\hat{\sigma}_{\hat{\alpha}_1}$	cov($\hat{\beta}_1, \hat{\alpha}_1$)	$t=1.5$ $\ln \hat{R}=1.639$ $\hat{\text{var}}_{\ln \hat{R}}=0.0004$	ICAM-1 $\hat{R}^*=4.8$ L CI _{95%} =4.5 U CI _{95%} =5.1
0.596	0.006	-13.490	0.152	-0.001		
$\hat{\beta}_2$						
0.635	0.007	-12.778	0.161	-0.001		
CD80						
$\hat{\beta}_1$	$\hat{\sigma}_{\hat{\beta}_1}$	$\hat{\alpha}_1$	$\hat{\sigma}_{\hat{\alpha}_1}$	cov($\hat{\beta}_1, \hat{\alpha}_1$)	$t=1.5$ $\ln \hat{R}=2.623$ $\hat{\text{var}}_{\ln \hat{R}}=0.001$	CD80 $\hat{R}^*=12.8$ L CI _{95%} =11.7 U CI _{95%} =13.9
0.668	0.011	-17.284	0.303	-0.003		
$\hat{\beta}_2$						
0.676	0.009	-14.877	0.205	-0.002		

the standard curve method may lead to significant inaccuracies when applied to C_t data produced on different days. This is consistent with our observation that less abundant mRNAs give rise to higher errors, since R is related to E raised to the power of C and the day effect will directly impact C . Ideally then, a standard curve for efficiency as well as all C_t data to be compared should be generated in a single day. However, this necessity significantly reduces the number of experimental conditions that can be evaluated versus any particular control condition.

3.6. Interpretation of relative abundance changes

Finally, we used the analytical method to compare mRNA abundances from freshly isolated resting cells with anti-CD40-activated cells and anti-IgM-activated cells. Again, β -actin and ICAM-1 mRNA abundances are elevated in the anti-CD40-activated RNA, 2.9- and 5.4-fold, respectively (Table 4). These values are only marginally different from those seen in Table 2 where RNA from anti-CD40-activated cells was compared to RNA from anti-IgM-activated cells. Thus, the relative mRNA abundance of β -actin and ICAM-1 should be virtually identical between resting and anti-IgM-activated cells, and, indeed, this is found to be

Table 3
Determination of accuracy

	α CD40/ α CD40
<i>The standard curve method</i>	
CD80	$\hat{R}^*=1.55 \pm 0.22$ (95% CI)
ST3Gal I	$\hat{R}^*=0.94 \pm 0.04$
ST3Gal V	$\hat{R}^*=0.69 \pm 0.15$
<i>The analytical method</i>	
CD80	$\hat{R}^*=1.03 \pm 0.19$
ST3Gal I	$\hat{R}^*=0.99 \pm 0.12$
ST3Gal V	$\hat{R}^*=1.03 \pm 0.13$

Table 4
Relative mRNA abundance

	α IgM/resting	α CD40/resting
Actin	$\hat{R}^*_{95\%}=1.0-1.2$	2.6-3.2
ICAM-1	$\hat{R}^*_{95\%}=0.96-1.1$	5.0-5.9
CD80	$\hat{R}^*_{95\%}=0.23-0.27$	2.8-3.3
ST3Gal I	$\hat{R}^*_{95\%}=0.26-0.30$	1.1-1.2
ST3Gal V	$\hat{R}^*_{95\%}=0.66-0.87$	0.57-0.74

the case (1.1 and 1.0, respectively). This does not suggest, however, that β -actin and ICAM-1 transcripts are not significantly increased following anti-IgM-mediated B cell activation. Rather, it suggests that β -actin and ICAM-1 transcription are more or less coordinately up-regulated with 18S rRNA synthesis, which is known to be dramatically increased following B cell activation (Dauphinais, 1981). That this is so may be evidenced by the difference in relative abundances of CD80 mRNA between resting cells and anti-CD40 (3-fold increase) and anti-IgM-activated cells (4-fold decrease). We conclude then that CD80 transcription is significantly enhanced in anti-CD40-activated cells, but is only negligibly increased (if at all) in anti-IgM-activated cells, thus accounting for the large difference (1280%) in the relative abundance of CD80 mRNA between anti-IgM- and anti-CD40-activated cells.

A similar result was seen when mRNA abundances of the sialyltransferase ST3Gal I were compared. Again, there was a significant loss of mRNA in anti-IgM, but not anti-CD40-activated cells compared to resting cells. This result is consistent with a significantly increased level of peanut agglutinin (PNA) binding to anti-IgM-stimulated cells compared to anti-CD40-stimulated and to resting cells (unpublished observations—data not shown). PNA binds to the disaccharide Gal β 1,3GalNAc-R, and this binding is blocked by the action of ST3Gal I (Priatel et al., 2000). These results are not, however, indicative of a general reduction in all mRNA abundances for anti-IgM-stimulated cells as the R^* values for actin and ICAM-1 are close to 1.0. Further, the R^* values for ST3Gal V are virtually identical between anti-IgM and anti-CD40-stimulated cells. All experiments reported here have been repeated several times with similar results.

4. Discussion

4.1. The methods

While several mathematical methodologies have been proposed for relative quantitative analysis of the data generated by real-time RT-PCR (Muller et al., 2002; Liu and Saint, 2002; Livak and Schmittgen, 2001; Gentle et al., 2001; Pfaffl, 2001), none have

provided a rigorous approach to the analysis of variance in their respective systems. We have also tried several other methods to derive efficiency values by nonlinear regression analysis including an exponential method (Liu and Saint, 2002) and both logistic and Gompertz-type equations (Schlereth et al., 1998) to model the PCR fluorescence growth curve; however, in our hands, no other curve-fitting method produces efficiency values as reliable as the standard curve (Pfaffl, 2001) and analytical (Gentle et al., 2001) methods. Further, by implementing new mathematical approaches developed for statistical rigor, we have been able to demonstrate that both methods are capable of producing precise results (Tables 1–4).

A number of considerations will enter into the decision of which of these procedures to adopt for use, and ease of implementation is certainly one. The standard curve method has the advantage of being the simplest to implement for data analysis, and a similar approach is currently available in at least two software packages (Muller et al., 2002; Sagner and Goldstein, 2001). However, as demonstrated in Table 3 of Results, this method may be less accurate under some conditions than the analytical method. Although the differences between the two protocols are slight when a highly transcribed mRNA like β -actin is examined, the differences become more significant as the transcripts become less abundant (compare actin and CD80 between Tables 1 and 2). We hypothesize, but have no way of proving, that since the analytical method is more accurate when comparing identical cDNAs (Table 3), it will also be more accurate when comparing non-identical cDNAs.

The standard curve method requires the use of multiple replicate samples to generate a standard curve for efficiency determination, and each amplicon requires its own standard curve. Further, the method assumes that amplicon amplification efficiency is invariant with respect to different DNA preparations, and this has been shown to be not always the case (Liu and Saint, 2002; Meijerink et al., 2001; and our unpublished observations). While the standard curves may be stored and applied to future determinations (Sagner and Goldstein, 2001), because of a significant 'day effect' (Fig. 1), the accuracy of the resultant calculations will always be in question (Table 3). This

is consistent with our observation that less abundant mRNAs give rise to higher errors using this method (Tables 1 and 2, and unpublished observations) as the increased number of cycles necessary for C_t determination increases any slight differences in initial conditions exponentially. Ideally then, a standard curve for efficiency as well as all C_t data to be compared should be generated in a single day. However, this necessity significantly reduces the number of sample conditions that can be evaluated versus any particular control condition unless analysis of the control condition is repeated each day that new sample conditions are analyzed.

We conclude that the analytical method gives a more accurate result because all the calculated values for any particular condition are derived from a single data set, and it should be chosen when data sets collected on different days are to be compared. It is important to note, however, that even when using the analytical method, certain data, i.e. target and reference data for any individual sample condition, should be collected simultaneously. This approach allows one to compile a relative expression database to which one may add any number of other sample conditions at any time, and any sample condition may then serve as the control condition.

When using the analytical method, it is also critical to remember that the slopes of the linear regression curves, which are the mathematical equivalents of E in Eq. (3) from Introduction, must be equal. This does not imply that the two mean slopes that will be averaged in Eq. (8) from Results must be identical; they rarely if ever will be (compare β_1 and β_2 in Table 2). Rather, it implies that the two data sets must be tested and found to be statistically indistinguishable to some degree of certainty (here, $p \geq 0.05$ is used). As suggested by Gentle et al. (2001), we use the method of Zar (1984) as implemented in GraphPad Prism for this determination. If this condition is met, then the results of the R^* determination made using our method of calculation will be dependable to the degree of certainty indicated by the upper and lower confidence intervals.

A number of relative quantitative real-time RT-PCR protocols have been developed using molecular beacon (Tyagi and Kramer, 1996) and TaqMan-type probes (Gibson et al., 1996). The use of such probes has been reported to have several advantages over

the use of SYBR Green I, including increased sensitivity and specificity, reduced primer-dimer formation, and the ability to multiplex reference and target genes in a single reaction tube (Bustin, 2000). Despite these obvious advantages, such probes also have several disadvantages that make the use of SYBR Green I attractive. These include the high cost of synthesizing individual TaqMan or molecular beacon probes for each gene assayed and the necessity of designing three functionally optimal, gene-specific probes for each gene assayed. Further, we have found that with the judicious selection of primer pairs, even comparatively rare mRNAs (as for the sialyltransferases) may be quantified using SYBR Green I. However, whether one uses SYBR Green I or TaqMan-type probes, the mathematical procedures described here are equally applicable and should give similar results.

4.2. The results

Activation of resting B cells with anti-CD40 antibodies but not with anti-IgM antibodies leads to significant aggregate formation in the cell cultures. Such aggregation has been attributed to intercellular interactions between ICAM-1 and activated LFA-1 molecules on the B cell surface (Barrett et al., 1991; Carlsson et al., 1993). Thus, our results showing that both ICAM-1 mRNA and protein are significantly more abundant in anti-CD40-activated cells relative to both anti-IgM-activated and resting cells (Fig. 4 and Tables 2 and 4) are completely consistent with the known role of this molecule in mediating the homotypic aggregation typical of CD40-activated B cells (Greicius et al., 1998). As it is well established that both ICAM-1 and LFA-1 require association with intracellular cytoskeletal microfilaments for full function (Carpen et al., 1992; Lub et al., 1997), an increase in β -actin mRNA abundance in anti-CD40 cells might be expected and is indeed observed (Table 4).

Anti-IgM-activated cells express ICAM-1 protein levels slightly greater than that seen on the resting cell surface (Fig. 4), and it has been demonstrated in reaggregation experiments that anti-IgM-activated cells are recruited into anti-CD40-generated clusters, even though they do not form clusters themselves (Cliff and Klaus, 2000). Surprisingly, ICAM-1 mRNA abundance is not greater in anti-IgM-activated cells

than in resting cells (Table 4). However, this does suggest that ICAM-1 transcription is coordinately up-regulated with rRNA synthesis. If such were not the case, ICAM-1 mRNA abundance would be expected to decrease with a resultant loss of the protein from the cell surface during blast formation (see below).

The relative abundance CD80 mRNA seems to be significantly higher in resting cells than in anti-IgM-stimulated cells (Table 4), neither of which express detectable protein (Fig. 3), and is only modestly higher in anti-CD40-activated cells, which express the protein, than it is in resting cells (Table 4). In time course studies, CD80 transcript abundance increases in anti-CD40-stimulated cells until 48 h then declines (data not shown). These results are consistent with the low level of the protein expression on the cell surface (Fig. 4). Further, it is known that triggering B cells through CD40 but not through cell surface IgM leads to CD80 expression (Lenschow et al., 1994; Goldstein et al., 1996). While the decrease in relative CD80 mRNA expression seen in anti-IgM-activated B cells could be due to some other factor such as mRNA destabilization, it is most likely due to increased abundance of rRNA which occurs without an accompanying increase in CD80 mRNA abundance. It is somewhat surprising that there are detectable CD80 transcripts in resting B cells as such transcripts have not been found in other resting cells inducible for CD80 expression (Fleischer et al., 1996). It is possible that the presence of CD80 transcripts is due to the small population of CD80 expressing cells in the initial resting cell preparation (Fig. 4); however, such cells do not make up more than 3–5% of the total cell population. On the other hand, this result demonstrates the importance of using RNA from highly purified cell populations for the preparation of the control and sample cDNA.

In contrast, the reduced abundance of ST3Gal I mRNA in anti-IgM-stimulated cells compared with resting or anti-CD40-stimulated cells correlates very well with an increased expression of PNA-binding carbohydrates on the B cell surface following anti-IgM stimulation (data not shown). It is well known from studies using transgenic KO mice that ST3Gal I is the principal glycosyltransferase responsible for blocking the expression of the PNA-binding phenotype in both T and B lymphocytes (Priatel et al., 2000). Although ST3Gal V mRNA abundance is also

slightly reduced in both anti-IgM and anti-CD40-stimulated cells, we have not attempted to determine whether there is any resultant phenotypic effect of this change.

4.3. Summary

Recently, several protocols for analyzing and validating data from real-time relative RT-PCR experiments have been published in peer-reviewed journals (Liu and Saint, 2002; Livak and Schmittgen, 2001; Pfaffl, 2001; Gentle et al., 2001). We have tested all of these approaches, developed new data analysis procedures for the two most promising of these methodologies, and generated data appropriate to assess both the accuracy and precision of both protocols. Using 18S rRNA as an internal reference, we have demonstrated that while both approaches to efficiency determination produce results that are precise, only the analytical method combined with our data analysis protocol produces consistently accurate, statistically verified results. We believe this is largely due to the existence of a day effect (Fig. 1), which introduces at least the potential for significant error into the standard curve method. Finally, we have demonstrated the utility and sensitivity of our approach by applying it to the analysis of changes in ICAM-1, CD80, and ST3Gal I mRNA abundance relative to 18S rRNA during differential B cell activation and shown that message transcript abundance closely correlates with cell surface expression of both protein and carbohydrate markers.

Acknowledgements

The authors thank Dr. Glen Collier for his critical reading of this manuscript and his helpful suggestions. This work was supported by grants to KSM from the National Institutes of Health (AI-41164) and from the Mervin Bovaird Center for Molecular Cell Biology and Biotechnology.

References

- Bagriacik, E.U., Miller, K.S., 1999. Cell surface sialic acid and the regulation of immune cell interactions: the neuraminidase effect reconsidered. *Glycobiology* 9, 267.

- Barrett, T.B., Shu, G., Clark, E.A., 1991. CD40 signaling activates CD11a/CD18 (LFA-1)-mediated adhesion in B cells. *J. Immunol.* 146, 1722–1729.
- Blaschke, V., Reich, K., Blaschke, S., Zipprich, S., Neumann, C., 2000. Rapid quantitation of proinflammatory and chemoattractant cytokine expression in small tissue samples and monocyte-derived dendritic cells: validation of a new real-time RT-PCR technology. *J. Immunol. Methods* 246, 79–90.
- Bustin, S.A., 2000. Absolute quantification of mRNA using real-time reverse transcription polymerase chain reaction assays. *J. Mol. Endocrinol.* 25, 169–193.
- Carlsson, M., Soderberg, O., Nilsson, K., 1993. Interleukin-4 (IL-4) enhances homotypic adhesion of activated B-chronic lymphocytic leukaemia (B-CLL) cells via a selective up-regulation of CD54. *Scand. J. Immunol.* 37, 515–522.
- Carpén, O., Pallai, P., Staunton, D.E., Springer, T.A., 1992. Association of intercellular adhesion molecule-1 (ICAM-1) with actin-containing cytoskeleton and alpha-actinin. *J. Cell Biol.* 118, 1223–1234.
- Cliff, J.M., Klaus, G.G., 2000. A method for investigating the role of homotypic adhesion in lymphocyte activation. *J. Immunol. Methods* 246, 51–59.
- Dauphinais, C., 1981. The control of ribosomal RNA transcription in lymphocytes. *Eur. J. Biochem.* 114, 487–492.
- Fleischer, J., Soeth, E., Reiling, N., Grage-Griebenow, E., Flad, H.D., Ernst, M., 1996. Differential expression and function of CD80 (B7-1) and CD86 (B7-2) on human peripheral blood monocytes. *Immunology* 89, 592–598.
- Freeman, W.M., Walker, S.J., Vrana, K.E., 1999. Quantitative RT-PCR: pitfalls and potential. *BioTechniques* 26, 112–125.
- Gentle, A., Anastasopoulos, F., McBrien, N.A., 2001. High-resolution semi-quantitative real-time PCR without the use of a standard curve. *BioTechniques* 31, 502–508.
- Gibson, U.E., Heid, C.A., Williams, P.M., 1996. A novel method for real time quantitative RT-PCR. *Genome Res.* 6, 995–1001.
- Goidin, D., Mamessier, A., Staquet, M., Schmitt, D., Berthier-Vergnes, O., 2001. Ribosomal 18s RNA prevails over glyceraldehyde-3-phosphate dehydrogenase and β -actin genes as internal standard for quantitative comparison of mRNA levels in invasive and noninvasive human melanoma cell subpopulations. *Anal. Biochem.* 295, 17–21.
- Goldstein, M.D., Debenedette, M.A., Hollenbaugh, D., Watts, T.H., 1996. Induction of costimulatory molecules B7-1 and B7-2 in murine B cells. The CBA/N mouse reveals a role for Bruton's tyrosine kinase in CD40-mediated B7 induction. *Mol. Immunol.* 33, 541–552.
- Greicius, G., Tamosiunas, V., Severinson, E., 1998. Assessment of the role of leucocyte function-associated antigen-1 in homotypic adhesion of activated B lymphocytes. *Scand. J. Immunol.* 48, 642–650.
- Hempel, D.M., Smith, K.A., Claussen, K.A., Perricone, M.A., 2002. Analysis of cellular immune responses in the peripheral blood of mice using real-time RT-PCR. *J. Immunol. Methods* 259, 129–138.
- Higuchi, R., Fockler, C., Dollinger, G., Watson, R., 1993. Kinetic PCR analysis: real-time monitoring of DNA amplification reactions. *Biotechnology* 11, 1026–1030.
- Kruse, N., Moriabadi, N.F., Toyka, K.V., Rieckmann, P., 2001. Characterization of early immunological responses in primary cultures of differentially activated human peripheral mononuclear cells. *J. Immunol. Methods* 247, 131–139.
- Lenschow, D.J., Sperling, A.I., Cooke, M.P., Freeman, G., Rhee, L., Decker, D.C., Gray, G., Nadler, L.M., Goodnow, C.C., Bluestone, J.A., 1994. Differential up-regulation of the B7-1 and B7-2 costimulatory molecules after Ig receptor engagement by antigen. *J. Immunol.* 153, 1990–1997.
- Liu, W., Saint, D.A., 2002. A new quantitative method of real time reverse transcription polymerase chain reaction assay based on simulation of polymerase chain reaction kinetics. *Anal. Biochem.* 302, 52–59.
- Livak, K.J., Schmittgen, T.D., 2001. Analysis of relative gene expression data using real-time quantitative PCR and the $2^{-\Delta\Delta C(T)}$ method. *Methods* 25, 402–408.
- Lub, M., van Kooyk, Y., van Vliet, S.J., Figdor, C.G., 1997. Dual role of the actin cytoskeleton in regulating cell adhesion mediated by the integrin lymphocyte function-associated molecule-1. *Mol. Biol. Cell* 8, 341–351.
- Meijerink, J., Mandigers, C., van de Locht, L., Tonnissen, E., Goodsaid, F., Raemaekers, J., 2001. A novel method to compensate for different amplification efficiencies between patient DNA samples in quantitative real-time PCR. *J. Mol. Diagnostics* 3, 55–61.
- Muller, P.Y., Janovjak, H., Miserez, A.R., Dobbie, Z., 2002. Processing of gene expression data generated by quantitative real-time RT-PCR. *BioTechniques* 32, 1372–1379.
- Mullis, K., Faloona, F., Scharf, S., Saiki, R., Horn, G., Erlich, H., 1986. Specific enzymatic amplification of DNA in vitro: the polymerase chain reaction. *Cold Spring Harbor Symp. Quant. Biol.* 51 (Pt. 1), 263–273.
- Overbergh, L., Valckx, D., Waer, M., Mathieu, C., 1999. Quantification of murine cytokine mRNAs using real time quantitative reverse transcriptase PCR. *Cytokine* 11, 305–312.
- Pfaffl, M.W., 2001. A new mathematical model for relative quantification in real-time RT-PCR. *Nucleic Acids Res.* 29, 2002–2007.
- Priatel, J.J., Chui, D., Hiraoka, N., Simmons, C.J., Richardson, K.B., Page, D.M., Fukuda, M., Varki, N.M., Marth, J.D., 2000. The ST3Gal-I sialyltransferase controls CD8⁺ T lymphocyte homeostasis by modulating O-glycan biosynthesis. *Immunity* 12, 273–283.
- Ririe, K.M., Rasmussen, R.P., Wittwer, C.T., 1997. Product differentiation by analysis of DNA melting curves during the polymerase chain reaction. *Anal. Biochem.* 245, 154–160.
- Sagner, G., Goldstein, C., 2001. Principles, workflows and advantages of the new LightCycler Relative Quantification Software. *Biochemica* 3, 15–17.
- Schlereth, W., Bassukas, I.D., Deubel, W., Lorenz, R., Hempel, K., 1998. Use of the recursion formula of the Gompertz function for the quantitation of PCR-amplified templates. *Int. J. Mol. Med.* 1, 463–467.
- Schmittgen, T.D., Zakrajsek, B.A., 2000. Effect of experimental treatment on housekeeping gene expression: validation by real-time, quantitative RT-PCR. *J. Biochem. Biophys. Methods* 46, 69–81.

- Spanakis, E., 1993. Problems related to the interpretation of autoradiographic data on gene expression using common constitutive transcripts as controls. *Nucleic Acids Res.* 21, 3809–3819.
- Thellin, O., Zorzi, W., Lakaye, B., De Bormain, B., Coumans, B., Hennen, G., Grisar, T., Igout, A., Heinen, E., 1999. Housekeeping genes as internal standards: use and limits. *J. Biotechnol.* 75, 291–295.
- Tyagi, S., Kramer, F.R., 1996. Molecular beacons: probes that fluoresce upon hybridization. *Nat. Biotechnol.* 14, 303–308.
- Wang, T., Brown, M.J., 1999. mRNA quantification by real time TaqMan polymerase chain reaction: Validation and comparison with RNase protection. *Anal. Biochem.* 269, 198–201.
- Wittwer, C.T., Herrmann, M.G., Moss, A.A., Rasmussen, R.P., 1997. Continuous fluorescence monitoring of rapid cycle DNA amplification. *BioTechniques* 22, 130–138.
- Zar, J.H., 1984. *Biostatistical Analysis*, 2nd ed. Prentice-Hall, Upper Saddle River, NJ.